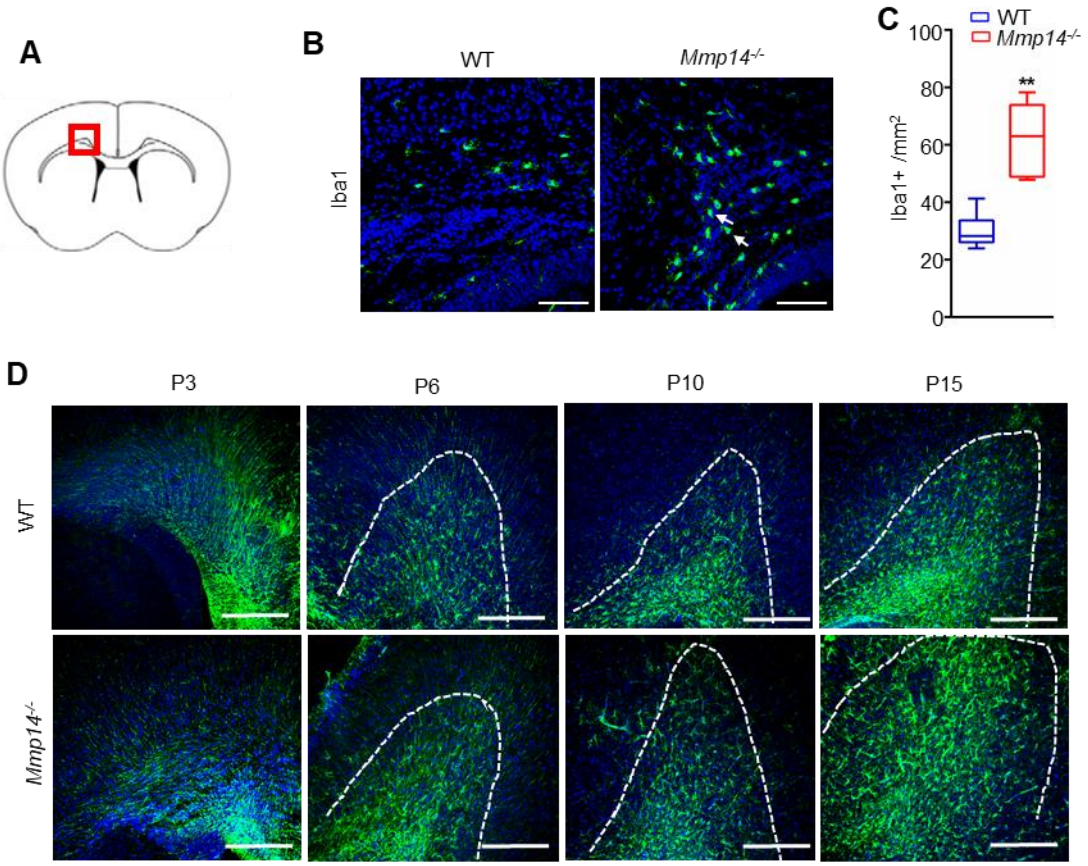

Supplemental Figure 1 (A). Diagram depicting the region in forebrain where the high-magnification photos were taken. **(B).** Immunofluorescent staining of Iba1 of coronal sections in the forebrains from wild-type and *Mmp14*$^{-/-}$ mice at P4. Arrows indicate microglia with amoeboid shapes. Scale bar, 100 μm. **(C).** Quantification of Iba1^{+} cells in **B** by two-tailed Student's *t* test. $^{**}p < 0.01$, n=3; Data represent mean ±SEM. **(D).** Representative images of immunofluorescent staining of GFAP in the forebrains from wild-type and *Mmp14*$^{-/-}$ mice at P3, P6, P10 and P15. Scale bar, 200 μm.

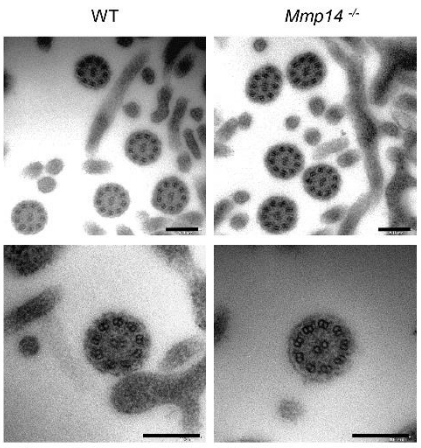

Supplemental Figure 2. Representative TEM analyses of '9+2' ultrastructure of motile cilia in ependymal cells in LV from wild-type and MT-MMP deficient mouse brains at P10. Scale bar, 200 nm.

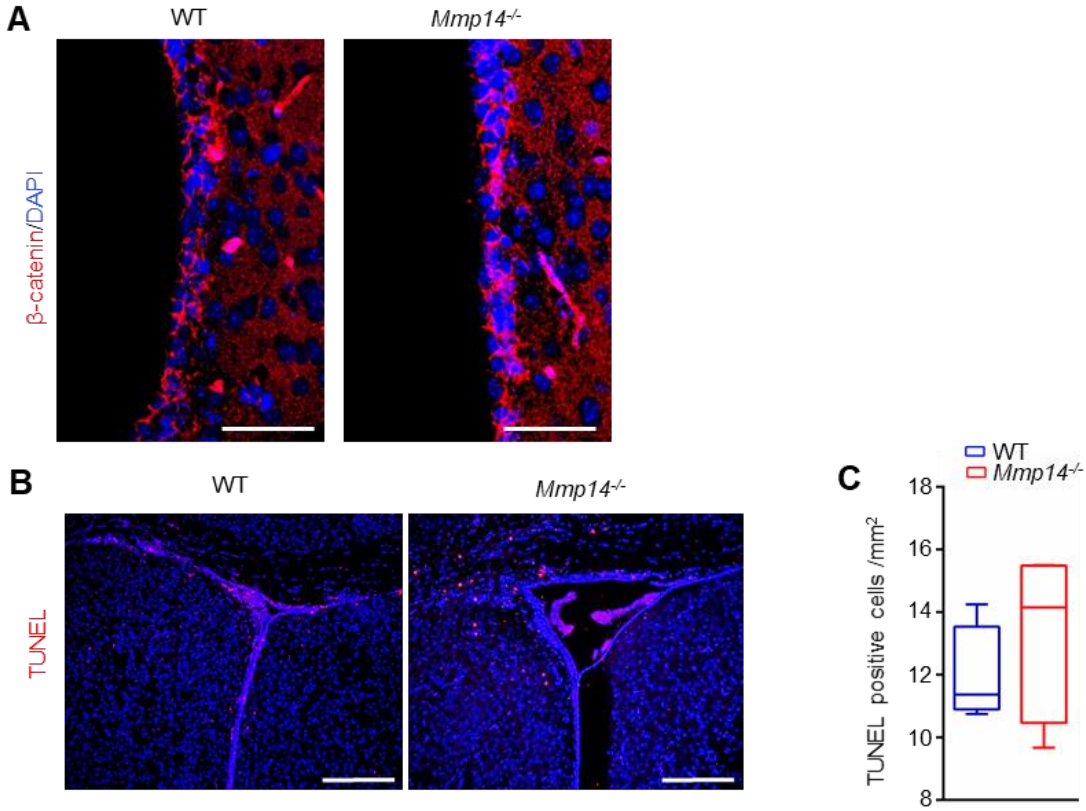

Supplemental Figure 3. (A). β-catenin staining of LV in WT and *Mmp14*$^{-/-}$ mice brain at P15. Scale bar, 50 μm. **(B).** TUNEL staining in VZ and SVZ regions of mouse brain at P15. Scale bar, 200 μm. **(C).** Quantification of VZ/SVZ ratio in **B** by two-tailed Student's *t* test, $p>0.05$, n=4; Data represent mean ±SEM.

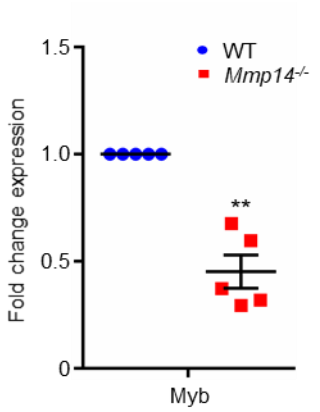

Supplemental Figure 4. Fold change in mRNA level of Myb in the wall of lateral ventricles between WT and *Mmp14*$^{-/-}$ mouse brains at P3. Levels of gene expression in WT samples were designated as 1. Statistical analysis performed by two-tailed Student's *t* test, $^{**}p < 0.01$, n=5.